Volume 5
Number 8
21 April 2023
Pages 2123–2362

Nanoscale Advances

rsc.li/nanoscale-advances

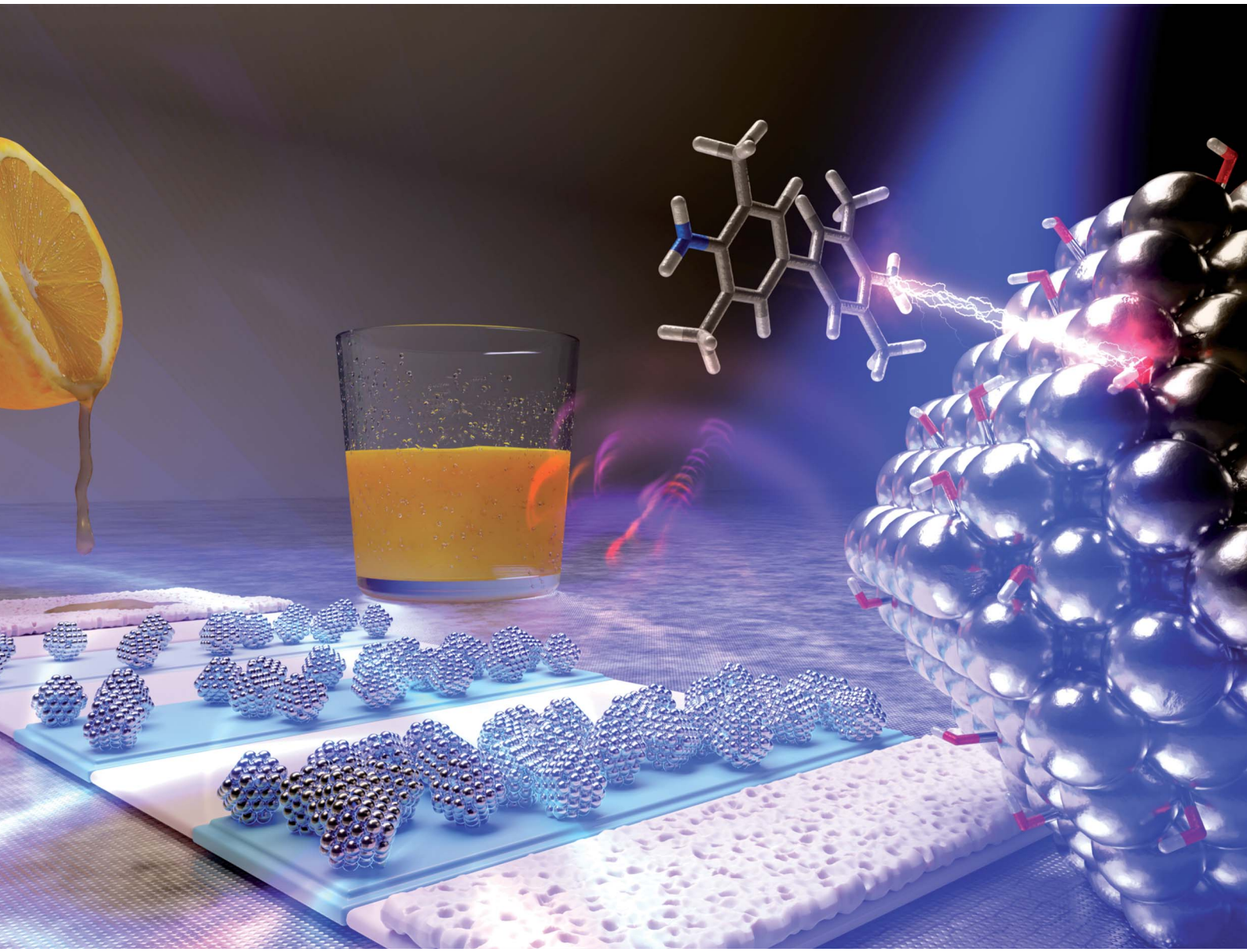

ISSN 2516-0230

ROYAL SOCIETY OF CHEMISTRY

COMMUNICATION

Pier Paolo Pompa *et al.*

A multi-line platinum nanozyme-based lateral flow device for the colorimetric evaluation of total antioxidant capacity in different matrices

NCNST

Nanoscale Advances

ROYAL SOCIETY OF CHEMISTRY

COMMUNICATION

View Article Online
View Journal | View Issue

Cite this: *Nanoscale Adv.*, 2023, **5**, 2167

A multi-line platinum nanozyme-based lateral flow device for the colorimetric evaluation of total antioxidant capacity in different matrices†

Anna Scarsi, [ab] Deborah Pedone[a] and Pier Paolo Pompa *[a]

Received 19th December 2022
Accepted 6th February 2023

DOI: 10.1039/d2na00931e

rsc.li/nanoscale-advances

The evaluation of Total Antioxidant Capacity (TAC), namely the complete pattern of antioxidant species in a complex medium, is of major interest in many fields ranging from health monitoring to quality control in the food industry. In this framework, point-of-care (POC) testing technologies are a promising diagnostic solution for rapid on-site analyses, unlike laboratory based-assays, which are often limited by centralized analyses, time-consuming and costly procedures, and invasiveness in the case of health diagnostics. In this work, we developed a POC methodology that evaluates TAC in different matrices, exploiting the peroxidase-like properties of 5 nm platinum nanoparticles (PtNPs), combined with a colorimetric paper-based device. Notably, we designed and optimized a multi-line PtNPs-based Lateral Flow Assay (LFA), which relies on three sequential test lines with increasing concentrations of platinum nanozymes, to get a non-invasive, accurate, and fast (10 minutes) colorimetric evaluation of the body TAC in saliva samples. Furthermore, we employed the device as a prototype of a quality control tool in the food industry, for the determination of the TAC in fruit juices.

1. Introduction

Nowadays, with the increase of lifestyle-related disorders, frequent preventive screenings are of great interest in healthcare.[1–3] In this context, point-of-care (POC) testing is raising consensus as a reliable alternative technology to instrumental-based assays,[4,5] which are often limited by costly and time-consuming procedures and need for centralized laboratories and specialized personnel.[6,7] POC testing allows the detection of several biomarkers in a variety of biological fluids, primarily serum and plasma, which include many relevant analytes at considerable concentrations.[8] Nevertheless, the use of blood involves some drawbacks, such as invasiveness, thus the employment of saliva as an alternative biological fluid for biomarkers' detection is gaining strong interest, thanks to its easy sampling and handling.[9–11] In recent years, in fact, a growing development of salivary POC testing has been proposed.[12–17]

In the context of early prevention, an interesting biomarker for monitoring the health condition of the organism is represented by the Total Antioxidant Capacity (TAC).[18,19] Currently, TAC can be measured by laboratory-based assays,[20] which however require long, expensive, and invasive procedures that prevent frequent screenings. To address this, some POC methods for the evaluation of antioxidant species have been recently published,[21–27] although most of them require an instrumental detection or could be improved in terms of stability and ease of reading.

In this work, we aimed to develop an effective antioxidant detection strategy, able to evaluate TAC in both food matrices and biological fluids (*i.e.*, saliva), by exploiting the nanozyme properties of platinum nanoparticles (PtNPs).[28] The use of nanozymes has recently seen an increasing diffusion in many applications.[29–31] Nanozymes are nanomaterials able to mimic natural enzymes, and thus they can be employed as powerful alternative tools, especially in uncontrolled non-biological environments, due to their unique features combining high catalytic efficiency with long-term stability at ambient conditions.[32] In this context, platinum nanoparticles are particularly effective peroxidase-like nanozymes, characterized by an easy and low-cost synthesis and high operational stability, thus making them interesting materials for POC diagnostics.[26,28,33–36] Furthermore, it has been demonstrated that PtNP size and shape can significantly modulate their catalytic properties, opening the possibility of tailored design and/or maximization of the catalytic activity of the nanoparticles.[37–40] In this application, we designed a hybrid system combining 5 nm Pt nanozymes with a paper-based device engineered with a multi-line Pt-based Lateral Flow Assay (LFA). Notably, this innovative

[a]*Nanobiointeractions & Nanodiagnostics, Istituto Italiano di Tecnologia (IIT), Via Morego 30, 16163-Genova, Italy. E-mail: pierpaolo.pompa@iit.it*

[b]*Department of Chemistry and Industrial Chemistry, University of Genova, Via Dodecaneso 31, 16146-Genova, Italy*

† Electronic supplementary information (ESI) available. See DOI: https://doi.org/10.1039/d2na00931e

strategy allows a semi-quantitative evaluation of TAC, providing a direct colorimetric readout within 10 minutes.

2. Results and discussion

2.1. Catalytic properties of 5 nm platinum nanoparticles

5 nm citrate-capped spherical platinum nanoparticles were selected as optimized peroxidase mimics to be employed in our colorimetric diagnostic assay (see Materials and methods for the synthesis details).[26] Fig. S1† illustrates the characterization of the as-synthesized nanoparticles. PtNPs were homogeneous in size and shape, as reported in the Transmission Electron Microscopy (TEM) image (Fig. S1a†) and size distribution plot (Fig. S1b†). Moreover, they presented a good dispersion in aqueous solution, with a narrow peak centered around 9 nm, as shown in the Dynamic Light Scattering (DLS) spectrum (Fig. S1c†). The high catalytic activity of the PtNPs is illustrated by the 5 min reaction kinetics relative to the oxidation of the chromogenic probe 3,3′,5,5′-tetramethylbenzidine (TMB) in presence of hydrogen peroxide (Fig. S1d†). Even at sub-micromolar concentrations, PtNPs showed a high peroxidase-like activity, as highlighted by the evident blue color generation reached after only 5 minutes.

2.2. PtNP-based LFA

The proposed LFA device is described in Fig. 1a. The device is based on a lateral flow strip, consisting in a sequence of pads (sample, conjugate, and absorbent pad) applied onto a nitrocellulose running membrane[41] (see Experimental for details). Unlike a standard LFA, which usually presents a single test line containing a probe (*e.g.*, an antibody) able to capture a gold nanoparticle-based detection bioreceptor to provide an optical readout,[41] our device exploits a different and innovative strategy. In particular, we designed a multi-line detection zone relying on three sequential PtNP-based test lines at increasing concentrations of nanozymes, which provide the colorimetric response of the assay by oxidizing TMB. The TMB probe is deposited onto the conjugate pad after the latter one is pre-treated with conjugate pad buffer (see Experimental for details). Untreated saliva samples, containing physiological antioxidants (AOX), are pre-mixed with hydrogen peroxide (H_2O_2) and directly deposited onto the sample pad, starting to flow through the strip. The sample reaches the conjugate pad and the reduced (colorless) form of TMB. When the flow gets to the detection area, the oxidation reaction takes place (Fig. 1b).[26,38] First, 5 nm platinum nanozymes activate H_2O_2, leading to the formation of hydroxyl radicals at their surface. Such radical species are responsible for the oxidation of TMB and the color change of the molecule from colorless to blue, providing the colorimetric response of the test. At the same time, antioxidants compete in the reaction mechanism at two levels. The major contribution to the competition is given by the direct interaction between AOX and hydroxyl radicals, which causes a saturation of active sites making them no longer available for the oxidative reaction with TMB. A secondary competitive mechanism is represented by the reverse reaction of TMB oxidation, carried out by AOX in excess. As an overall result, a minor quote of TMB is oxidized, and therefore the blue color intensity is inversely proportional to the concentration of AOX in the saliva samples.

We exploited such mechanisms to develop a detection zone able to provide a semi-quantitative readout of the antioxidant content, realizing three test lines at increasing concentration of Pt nanozymes (Fig. 1c). Such sensing design allowed us to

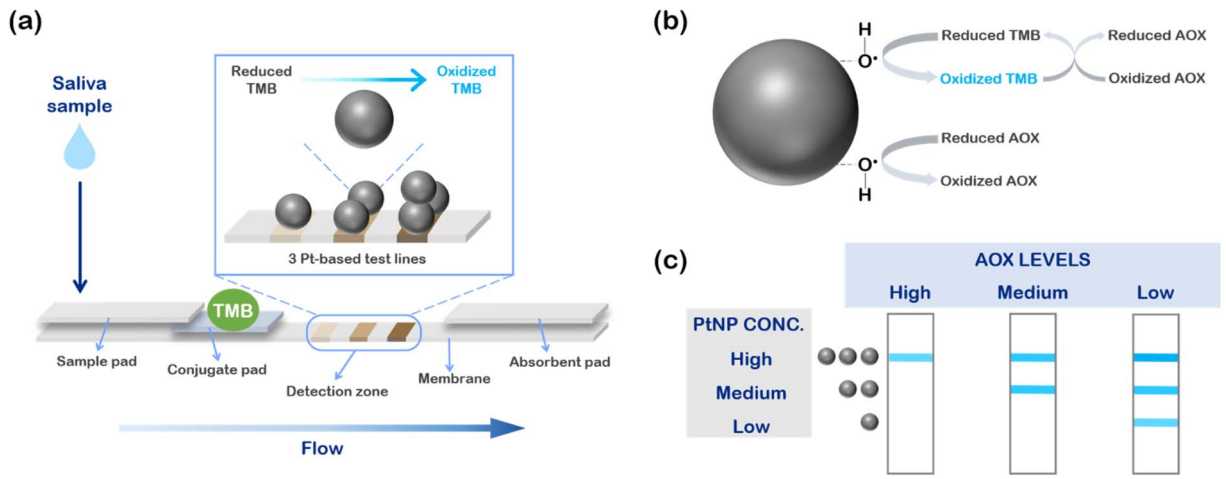

Fig. 1 Design and detection mechanism of the Pt nanozyme-based LFA. (a) Scheme of the device, based on three test lines at increasing concentrations of PtNPs. The antioxidant species in saliva compete with the chromogenic probe at the detection zone, preventing the oxidation of TMB and providing the color change of a number of test lines inversely proportional to the amount of AOX molecules. H_2O_2 is added to the saliva sample in advance, leading to the formation of the hydroxyl radicals at the nanoparticles' surface and leading to the oxidation of the reduced species (b). Antioxidants compete with TMB primarily directly interacting with hydroxyl radicals, and secondarily by reversing the TMB oxidation reaction. (c) As a result, a sample with a high amount of antioxidants shows one single test line, corresponding to the higher concentration of PtNPs. A medium TAC sample presents two test lines, while a sample with a low antioxidants level shows all the three test lines, since the amount of antioxidants is too small to compete with TMB.

discriminate between three classes of samples based on their antioxidant levels. In a sample with a high antioxidant content, AOX species are in large excess with respect to hydroxyl radicals, thus, at the first two lines, where PtNP concentrations are, respectively, low and medium, antioxidants win the competition and the two test lines result colorless. Conversely, when the PtNP amount is high (third test line), there are still hydroxyl radicals available to oxidize TMB, and so the line appears blue. Therefore, a sample with high antioxidant level will color just one test line, the one with the higher concentration of PtNPs. Progressively decreasing the AOX levels, the competition is in favor of TMB, and the test lines with less PtNPs will assume a blue color as well. In particular, a medium sample will color two lines, whilst a sample with a low antioxidant content will color all the three test lines.

A few examples of platinum-based LFAs have been recently reported in the literature, however in these systems, based on immunodetection strategies, platinum is usually employed in classical LFA configurations as a signal enhancer of other types of nanoparticles, primarily gold nanoparticles, exploiting the formation of Au@Pt nanoparticles and/or using chromogenic probes, such as TMB, to improve the sensitivity of the assay.[34,35,42–50] Yet, in our work, the detection mechanism is completely different, since it exploits a "competitive" catalytic reaction at the test line, with no antibodies or recognition/capturing species.

2.3. LFA strip optimization

Since we aimed at a rapid colorimetric detection, we first screened various types of nitrocellulose membranes with different pore sizes, and then selected a large pore size one, able to provide a faster run of the biological sample. Regarding the design of the detection zone, we tested and optimized a wide range of PtNP concentrations (from 1 to 100 ppm) in order to have a selective response within the dynamic range of salivary antioxidants, getting a final configuration of three Pt-based test lines (4, 25 and 100 ppm), deposited at a mutual distance of 4 mm by using an automatic dispenser (see Experimental for details).

Afterwards, we investigated the possible effect of pads' pre-treatments on the homogeneity and performance of the flow along the device.[41] We found the best condition by treating the sample pad with a sodium dodecyl sulfate-based buffer (see Experimental for details). Furthermore, to ensure a homogeneous coloring of the detection zone, without smears between the various test lines, we decided to first pre-treat the conjugate pad with a proper buffer (based on sucrose and tween), and then soak it with TMB stock solution (see Experimental for details).

2.4. Evaluation of antioxidant species in saliva samples

The optimized strips were then employed to evaluate the antioxidant content in saliva samples, collected from healthy donors. The TAC level of each sample was first evaluated through a reference instrumental method, namely UV-vis spectrophotometry (see Experimental for details), leading to the identification of three main classes, each one corresponding to the maximum absorbance level of oxidized TMB evaluated at 652 nm (Abs_{652}).[26] We related samples with $Abs_{652} \approx 0.2$ to a high antioxidant content, samples with $Abs_{652} \approx 0.5$ to a medium antioxidant content, and samples with $Abs_{652} \approx 0.8$ to a low antioxidant content.

Taking into the account these reference values, we preliminarily performed a proof-of-concept experiment employing a salivary sample with a medium antioxidant content (Fig. 2). To simulate the entire dynamic range of antioxidant species, we divided the sample in three aliquots after the pre-filtration step. One aliquot was diluted with water ("Diluted saliva"), to simulate a sample with a low antioxidant content, while in another

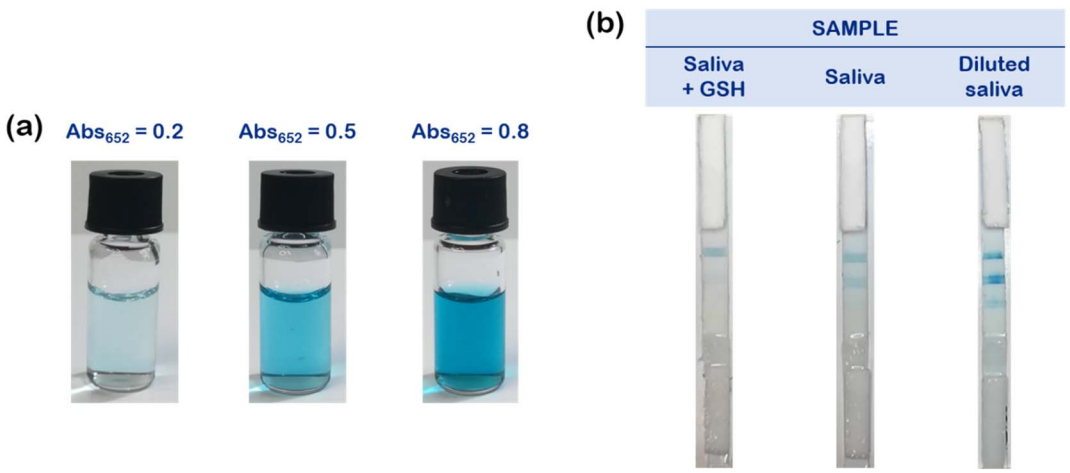

Fig. 2 Proof-of-concept experiment to determine antioxidant content in saliva samples. (a) Vials showing the visual results of the UV-vis spectrophotometry analysis performed on the considered samples. As illustrated, the intensity of the blue color increases while decreasing the antioxidant content, in agreement with the Abs_{652} value on top of each vial. (b) Representative pictures of the three devices evaluated at 10 minutes. The number of lines increases while decreasing the antioxidant levels in the samples. "Saliva + GSH": physiological saliva sample with an addition of 10 mM glutathione; "Saliva": physiological saliva sample without further modifications; "Diluted saliva": physiological saliva sample diluted with 90% of pure water.

one we added a glutathione (GSH) stock solution, up to a final concentration of 10 mM ("Saliva + GSH"), which is an appropriate content to simulate a high AOX saliva.[26] The third aliquot was left as it was ("Saliva"). The antioxidant content of the samples was first evaluated instrumentally as mentioned above (Fig. 2a). Then, we added H_2O_2, and we started the test depositing 100 μL onto the sample pad (Fig. 2b). At 10 minutes, we evaluated the results by a simple visual inspection and through a standard smartphone camera.

Notably, for the sample "Saliva + GSH", having a high antioxidant content, a single test line became blue, corresponding to the higher PtNPs' concentration (100 ppm). The sample with a medium antioxidant content ("Saliva") resulted in two colored test lines (100 and 25 ppm), while "Diluted saliva" (with a low antioxidant content) elicited the colorimetric detection of all the three test lines.

After assessing the correct working mechanism in a proof-of-principle experiment, we evaluated the TAC levels of different saliva samples, in a real case application. In order to minimize viscosity variations among the different samples, achieving a homogeneous flow with a reproducible test response, we setup a simple and rapid pre-filtration step (no other sample pre-treatments or purification necessary), using cellulose acetate syringe filters (0.2 μm pore size). This easy and fast procedure (the entire process takes about 30 seconds) allowed us to remove mucins from saliva in a single-step, requiring about 1 mL of sample.[51]

As described above, we first identified the three classes of AOX levels based on the spectrophotometric measurements using 9 saliva samples (Fig. 3a). Remarkably, using the multi-line device, we obtained three samples with a high antioxidant content (samples 1, 2 and 3, showing one main test line), three samples characterized by a medium TAC level (samples 4, 5 and 6, with two test lines highlighted), and three samples with low AOX levels (samples 7, 8 and 9, coloring all the three test lines), in line with the instrumental readouts (Fig. 3a). Moreover, exploiting smartphone pictures of these samples, we performed a quantitative analysis of the detection zones, calculating the red (R) value (complementary color of blue)[52,53] for each test line (Fig. 3b). The graph highlights that signals corresponding to R value below 20 (dashed reference line) can be considered as noise, in fact such test lines were typically

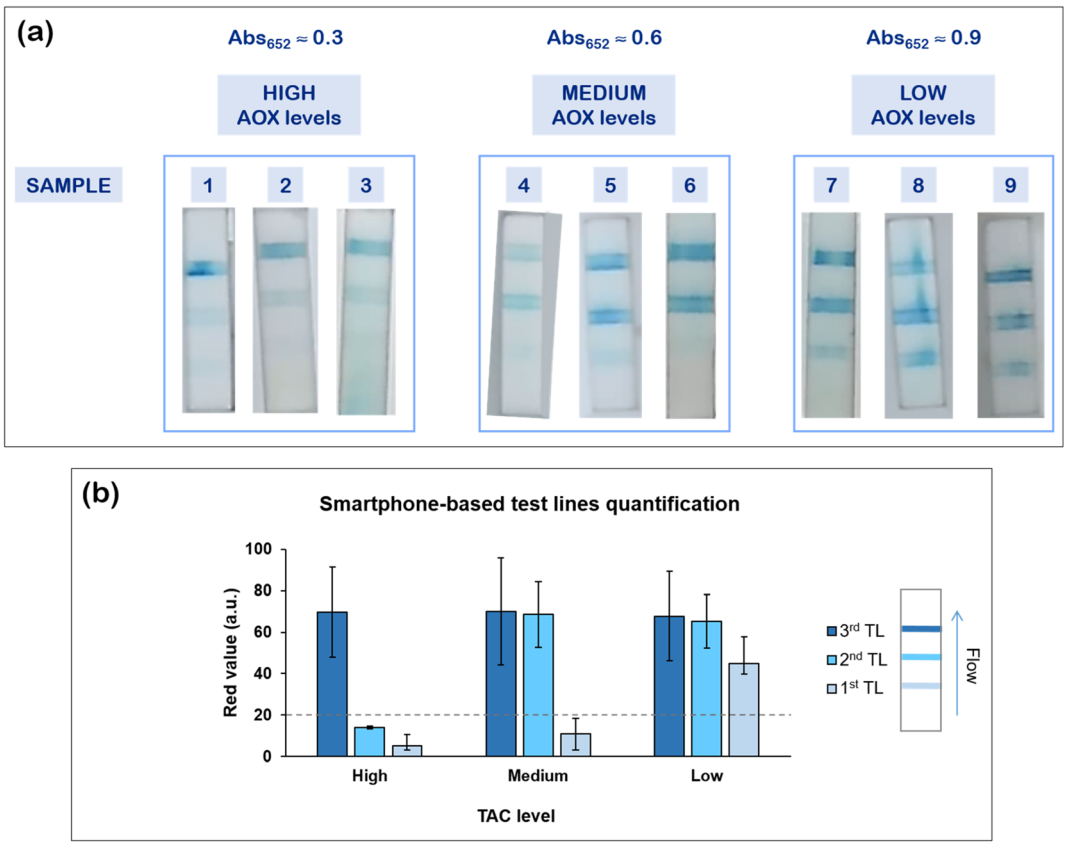

Fig. 3 Body TAC assessment in real saliva samples. (a) The 9 samples evaluated were divided into three groups (based on the Abs_{652} level), each one characterized by a different amount of antioxidant species (high, medium, and low AOX levels). The number of test lines is clearly visible on each device. (b) ImageJ analysis of the 9 samples reporting the average values of the red coordinate (complementary of the blue color) and the relative standard deviations corresponding to the first, second, and third test line (TL) of each group (samples with high, medium, and low TAC level, respectively). In the "low" group, the red value relative to the first test line has lower intensity because the concentration of PtNPs used was very small (4 ppm), in order to better discriminate the "medium" group from the "low" group. The dashed line serves as a reference to better highlight the noise threshold.

negligible upon visual inspection. On the contrary, such analysis clearly indicates that salivary samples with high (1, 2, 3), medium (4, 5, 6), and low (7, 8, 9) TAC levels respectively displayed one, two, or three positive test lines, all of them characterized by an intense red value (the 1st test line is less intense, due to the lower concentration of PtNPs employed, which enabled the assay discrimination). We thus confirmed the reliability and the robustness of the proposed POC device for the rapid and easy colorimetric evaluation of the body TAC through saliva samples (also *via* automated smartphone-based readout), in agreement with the antioxidant levels measured by UV-vis spectrophotometry.

2.5. Evaluation of antioxidant species in fruit juices

Given the relevance of antioxidant species not only in biological fluids, but also in other fields such as nutrition and food industry,[54–57] we exploited our device to evaluate the antioxidant content of some commercially available fruit juices. Eight juices were preliminary tested for their antioxidant content through UV-vis spectrophotometry as mentioned before, and we selected three types of juices based on their Abs_{652} value: "red orange juice" had a high antioxidant content, "peach juice" had a medium antioxidant content, and "apricot juice" was characterized by a low antioxidant content. We employed these three samples in a real case experiment (Fig. 4).

Before performing the test, we first optimized the concentration of the Pt nanozymes at the detection zone for this application, selecting 2, 15, and 100 ppm as the optimal conditions to have an efficient discrimination between the different juice samples. Then, we diluted each juice in water, to minimize the viscosity and color differences among the different fluids. After mixing with H_2O_2, we deposited 100 μL of the test juice onto the sample pad and we evaluated the results at 10 minutes, as previously reported. Fig. 4 shows a representative picture of the devices at the end of the test. Also in this case, the catalytic multi-line LFA proved effective in discriminating AOX levels in juice matrices, with the red orange juice (high antioxidant content) coloring one test line, the medium sample (peach juice) coloring two test lines, and the apricot juice (low antioxidant level) coloring all the three test lines. Hence, this method allowed fast and easy characterization of fruit juices based on their antioxidant contents, representing a promising POC technique in quality control procedures.

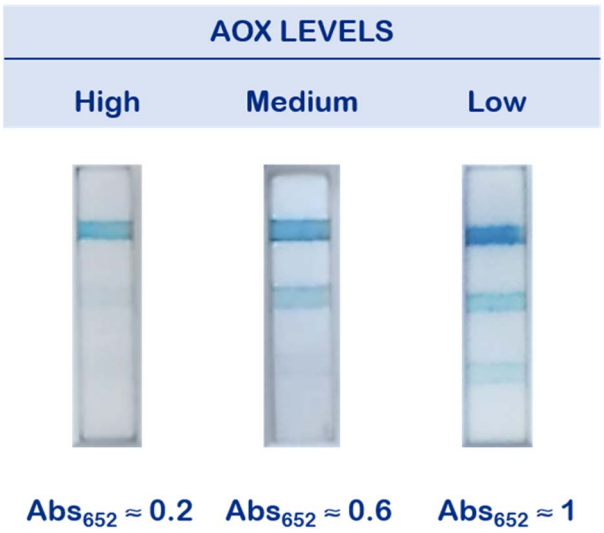

Fig. 4 Antioxidant levels evaluation in fruit juices. Representative pictures of the devices after been tested with the three fruit juice's samples. One, two and three blue test lines are respectively shown for high, medium and low AOX levels samples. Abs_{652} levels are respectively reported for each sample: red orange ("High"), $Abs_{652} \approx 0.2$; peach ("Medium"), $Abs_{652} \approx 0.6$; apricot ("Low"), $Abs_{652} \approx 1$.

3. Conclusions

In this work, we have developed an innovative multi-line PtNPs-based lateral flow device for the evaluation of antioxidant species in saliva and fruit juice samples. We exploited the peroxidase-like properties of small spherical platinum nanoparticles to obtain a direct optical detection, based on the coloring of a variable number of positive blue test lines. We were able to identify three main classes of samples, based on their antioxidant levels (high, medium, and low), which were validated through comparison with reference instrumental detection, *i.e.* UV-vis spectrophotometry. The POC device was tested on real saliva and juice samples, requiring fast and easy sample pre-treatments, and showing reproducibility and robustness in the tested conditions. The results were rapidly evaluated after 10 minutes by using naked-eye inspection or a smartphone readout. The proposed technology is the first example of multi-line catalytic Pt-based LFA and could be a promising POC approach for the visual evaluation of antioxidant levels in different matrices. Although the designed multi-line system has some limitations in terms of resolution, it can provide a wide dynamic range and can be quite easily adapted to several types of non-invasive biological fluids or food matrices, requiring minimal pre-analytical steps, thus opening interesting perspectives for applications in POC wellness monitoring or as a quality control tool in food industry and nutrition.

4. Materials and methods

4.1. Chemicals and materials

All chemicals and reagents employed were of high technical grade, stored following vendor recommendations, and directly used with no further purification.

Chloroplatinic acid hexahydrate ($H_2PtCl_6 \cdot 6H_2O$, BioXtra), sodium borohydride (H_4BNa, granular, 99.99% trace metal basis), sodium citrate tribasic dihydrate ($C_6H_5Na_3O_7 \cdot 2H_2O$, BioUltra, for molecular biology, ≥99.5%), hydrogen peroxide solution (H_2O_2, 30% (w/w) in H_2O, contains stabilizer), L-glutathione reduced ($C_{10}H_{17}N_3O_6S$, ≥98.0%), phosphate buffered saline (tablet), sucrose ($C_{12}H_{22}O_{11}$, BioUltra, for molecular biology, ≥99.5% (HPLC)), Tween 20 ($C_{58}H_{114}O_{26}$, viscous liquid), sodium dodecyl sulfate ($C_{12}H_{25}O_4S \cdot Na$, BioUltra, for molecular biology, ≥99.0% (GC)), Amicon Ultra-15 Centrifugal Filter Unit (Ultracel-50 regenerated cellulose membrane, 15 mL sample volume) were purchased from Merck (Sigma-Aldrich).

3,3′,5,5′-Tetramethylbenzidine (TMB) was obtained from Kem-En-Tec Diagnostics.

Sample pad (grade 319, composition cotton fibers), conjugate pad (grade 8980, composition chopped glass w/binder) and absorbent pad (grade 440, composition cotton/glass blend) were purchased from Ahlstrom-Munksjö. Nitrocellulose membrane (UniSart® CN 95 polyester backing 100 μm, 25 mm × 100 m) was purchased from Sartorius.

Distilled, deionized water (Millipore, Milli-Q system) was used for all solution preparation.

4.2. Synthesis and characterization of platinum nanoparticles

Spherical 5 nm citrate-capped PtNPs were synthesized by wet chemical reduction in water, following a previously reported protocol.[33] PtNP monodispersity and stability were evaluated by Transmission Electron Microscopy (TEM, JEOL JE-1011 microscope with thermionic source (W filament). Accelerating voltages: 100 kV; conventional TEM imaging: bright field; TEM resolution = 4.0 Å (100 kV)) and Dynamic Light Scattering (DLS, Zetasizer Nano Range (Malvern-PANalytical)). PtNP diameter was measured considering at least 150 nanoparticles analyzing TEM images with ImageJ software (NIH).

4.3. Lateral flow strip preparation

The sample pad was pre-treated with sample pad buffer (PBS 10 mM pH 7.4, 0.05% SDS) and let dry for 1 hour at 37 °C, and then for 2 hours under vacuum.

The conjugate pad was pre-treated with conjugate pad buffer (PBS 10 mM pH 7.4, 2.5% sucrose, 0.25% Tween 20) and let dry for at least 1 hour under vacuum. Then, it was soaked with TMB (stock solution) and let dry again for 1 hour under vacuum and in absence of light, to preserve the TMB molecule. The three test lines were obtained by striping three PtNP solutions at different concentration onto the nitrocellulose membrane 4 mm one from another, by using a Biodot XYZ S-series V3.11 (dispense rate of 0.625 μL cm^{-1} and a speed of 50 mm s^{-1}). The combinations "low-medium-high" of PtNP concentrations were 4–25–100 ppm (μg mL^{-1}) for the evaluation of antioxidants in saliva samples, and 2–15–100 ppm (μg mL^{-1}) for the evaluation of antioxidants in fruit juices.

4.4. Test procedure

4.4.1. Saliva samples preparation. Unstimulated saliva samples were collected from healthy donors at least 1 hour after performing oral care procedures, eating and drinking.[17] Their antioxidant content was determined by UV-vis spectrophotometry (Thermo Fisher NanoDrop®, wavelength accuracy ± 1 nm, absorbance accuracy 3% at 0.74 Abs @ 350 nm) reading TMB absorbance at 652 nm following an established protocol.[26] After that, the samples were first filtered to remove mucins (0.2 μm acetate cellulose syringe filters were used) and then diluted 1 : 1.2 in 1 M H_2O_2. In the proof-of-concept experiment of Fig. 2, the high AOX content case was obtained by spiking a GSH standard solution after the filtration to get a final GSH concentration of 10 mM, while the low AOX level case was simulated diluting saliva at 90% in pure water. Regarding the real cases application (Fig. 3), the samples were tested as they were after the filtration step. The red value analysis on the smartphone pictures of Fig. 3a was performed using ImageJ software (NIH).

4.4.2. Fruit juice samples preparation. Three fruit juices (red orange, peach and apricot, respectively) were bought to a local supermarket and their antioxidants level was initially determined by UV-vis spectrophotometry as mentioned above. Then, they were first diluted 1 : 4 in pure water (to homogenize the viscosity in each juice) and then 1 : 1.2 in 0.25 M H_2O_2.

4.4.3. Test run and results evaluation. 100 μL of each sample (both saliva and juice samples) were added onto the sample pad and the results were assessed at 10 minutes. Pictures were acquired using a Huawei P10-lite smartphone camera in non-controlled light conditions, to better simulate a real utilization of the device.

Ethical statement

All subjects gave written informed consent for the inclusion in this study. The protocol of the research study was approved by the Ethical Committee of Regione Liguria (405/2020-DB id 10787).

Conflicts of interest

The authors declare no conflicts of interest.

Acknowledgements

This work has been partially supported by Italian Space Agency (ASI) through the MARS-PRE Project. The authors gratefully acknowledge Valentina Mastronardi and Mauro Moglianetti for useful discussions and help during experiments.

References

1 M. Sharma and P. K. Majumdar, Occupational lifestyle diseases: An emerging issue, *Indian J. Occup. Environ. Med.*, 2009, **13**(3), 109–112.
2 M. Fatma Al-Maskari, *LIFESTYLE DISEASES: An Economic Burden on the Health Services*, **https://www.un.org/en/chronicle/article/lifestyle-diseases-economic-burden-health-services**.
3 Office of Disease Prevention and Health Promotion, *U. S. D. o. H. a. H. S. Preventive Care*, **https://health.gov/healthypeople/objectives-and-data/browse-objectives/preventive-care**.
4 C. Dincer, R. Bruch, E. Costa-Rama, M. T. Fernández-Abedul, A. Merkoçi, A. Manz, G. A. Urban and F. Güder, Disposable Sensors in Diagnostics, Food, and Environmental Monitoring, *Adv. Mater.*, 2019, **31**(30), 1806739.
5 L. Boselli, T. Pomili, P. Donati and P. P. Pompa, Nanosensors for Visual Detection of Glucose in Biofluids: Are We Ready for Instrument-Free Home-Testing?, *Materials*, 2021, **14**(8), 1978.

6 A. Sharma, A. I. Y. Tok, P. Alagappan and B. Liedberg, Point of care testing of sports biomarkers: Potential applications, recent advances and future outlook, *TrAC, Trends Anal. Chem.*, 2021, **142**, 116327.
7 B. Heidt, W. F. Siqueira, K. Eersels, H. Diliën, B. van Grinsven, R. T. Fujiwara and T. J. Cleij, Point of Care Diagnostics in Resource-Limited Settings: A Review of the Present and Future of PoC in Its Most Needed Environment, *Biosensors*, 2020, **10**(10), 133.
8 S. M. Yang, S. Lv, W. Zhang and Y. Cui, Microfluidic Point-of-Care (POC) Devices in Early Diagnosis: A Review of Opportunities and Challenges, *Sensors*, 2022, **22**(4), 1620.
9 I. T. Gug, M. Tertis, O. Hosu and C. Cristea, Salivary biomarkers detection: Analytical and immunological methods overview, *TrAC, Trends Anal. Chem.*, 2019, **113**, 301–316.
10 G. Giacomello, A. Scholten and M. K. Parr, Current methods for stress marker detection in saliva, *J. Pharm. Biomed. Anal.*, 2020, **191**, 113604.
11 R. S. Khan, Z. Khurshid and F. Yahya Ibrahim Asiri, Advancing Point-of-Care (PoC) Testing Using Human Saliva as Liquid Biopsy, *Diagnostics*, 2017, **7**(3), 39.
12 S. Williamson, C. Munro, R. Pickler, M. J. Grap and R. K. Elswick Jr, Comparison of biomarkers in blood and saliva in healthy adults, *Nursing Research and Practice*, 2012, **2012**, 246178.
13 V. C. Francavilla, F. Vitale, M. Ciaccio, T. Bongiovanni, C. Marotta, R. Caldarella, L. Todaro, M. Zarcone, R. Muratore, C. Bellia, G. Francavilla and W. Mazzucco, Use of Saliva in Alternative to Serum Sampling to Monitor Biomarkers Modifications in Professional Soccer Players, *Front. Physiol.*, 2018, **9**, 1828.
14 J. LeGoff, S. Kernéis, C. Elie, S. Mercier-Delarue, N. Gastli, L. Choupeaux, J. Fourgeaud, M.-L. Alby, P. Quentin, J. Pavie, P. Brazille, M. L. Néré, M. Minier, A. Gabassi, C. Leroy, B. Parfait, J.-M. Tréluyer and C. Delaugerre, Evaluation of a saliva molecular point of care for the detection of SARS-CoV-2 in ambulatory care, *Sci. Rep.*, 2021, **11**(1), 21126.
15 M. Yamaguchi, Salivary Sensors in Point-of-Care Testing, *Sensor. Mater.*, 2010, **22**, 143–153.
16 H. Torné-Morató, P. Donati and P. P. Pompa, Nanoplasmonic Strip Test for Salivary Glucose Monitoring, *Nanomaterials*, 2022, **12**(1), 105.
17 T. Pomili, P. Donati and P. P. Pompa, Paper-Based Multiplexed Colorimetric Device for the Simultaneous Detection of Salivary Biomarkers, *Biosensors*, 2021, **11**(11), 443.
18 A. Ghiselli, M. Serafini, F. Natella and C. Scaccini, Total antioxidant capacity as a tool to assess redox status: critical view and experimental data, *Free Radicals Biol. Med.*, 2000, **29**(11), 1106–1114.
19 C. P. Rubio, J. Hernández-Ruiz, S. Martinez-Subiela, A. Tvarijonaviciute and J. J. Ceron, Spectrophotometric assays for total antioxidant capacity (TAC) in dog serum: an update, *BMC Vet. Res.*, 2016, **12**(1), 166.
20 R. L. Prior and G. Cao, In vivo total antioxidant capacity: comparison of different analytical methods1, *Free Radicals Biol. Med.*, 1999, **27**(11), 1173–1181.
21 S. Sateanchok, S. Wangkarn, C. Saenjum and K. Grudpan, A cost-effective assay for antioxidant using simple cotton thread combining paper based device with mobile phone detection, *Talanta*, 2018, **177**, 171–175.
22 C. Puangbanlang, K. Sirivibulkovit, D. Nacapricha and Y. Sameenoi, A paper-based device for simultaneous determination of antioxidant activity and total phenolic content in food samples, *Talanta*, 2019, **198**, 542–549.
23 T. G. Choleva, F. A. Kappi, D. L. Giokas and A. G. Vlessidis, Paper-based assay of antioxidant activity using analyte-mediated on-paper nucleation of gold nanoparticles as colorimetric probes, *Anal. Chim. Acta*, 2015, **860**, 61–69.
24 K. Sirivibulkovit, S. Nouanthavong and Y. Sameenoi, Paper-based DPPH Assay for Antioxidant Activity Analysis, *Anal. Sci.*, 2018, **34**(7), 795–800.
25 T. Piyanan, A. Athipornchai, C. S. Henry and Y. Sameenoi, An Instrument-free Detection of Antioxidant Activity Using Paper-based Analytical Devices Coated with Nanoceria, *Anal. Sci.*, 2018, **34**(1), 97–102.
26 D. Pedone, M. Moglianetti, M. Lettieri, G. Marrazza and P. P. Pompa, Platinum Nanozyme-Enabled Colorimetric Determination of Total Antioxidant Level in Saliva, *Anal. Chem.*, 2020, **92**(13), 8660–8664.
27 E. Ragusa, V. Mastronardi, D. Pedone, M. Moglianetti, P. P. Pompa, R. Zunino and P. Gastaldo, Random Weights Neural Network for Low-Cost Readout of Colorimetric Reactions: Accurate Detection of Antioxidant Levels, *Advances in System-Integrated Intelligence*, ed. M. Valle, D. Lehmhus, C. Gianoglio, E. Ragusa, L. Seminara, S. Bosse, A. Ibrahim and K.-D. Thoben, Springer International Publishing, Cham, 2023, pp. 95–104.
28 D. Pedone, M. Moglianetti, E. De Luca, G. Bardi and P. P. Pompa, Platinum nanoparticles in nanobiomedicine, *Chem. Soc. Rev.*, 2017, **46**(16), 4951–4975.
29 J. Wu, X. Wang, Q. Wang, Z. Lou, S. Li, Y. Zhu, L. Qin and H. Wei, Nanomaterials with enzyme-like characteristics (nanozymes): next-generation artificial enzymes (II), *Chem. Soc. Rev.*, 2019, **48**(4), 1004–1076.
30 Z. Wang, R. Zhang, X. Yan and K. Fan, Structure and activity of nanozymes: Inspirations for de novo design of nanozymes, *Mater. Today*, 2020, **41**, 81–119.
31 Y. Huang, J. Ren and X. Qu, Nanozymes: Classification, Catalytic Mechanisms, Activity Regulation, and Applications, *Chem. Rev.*, 2019, **119**(6), 4357–4412.
32 X. Ren, D. Chen, Y. Wang, H. Li, Y. Zhang, H. Chen, X. Li and M. Huo, Nanozymes-recent development and biomedical applications, *J. Nanobiotechnol.*, 2022, **20**(1), 92.
33 M. Moglianetti, E. De Luca, D. Pedone, R. Marotta, T. Catelani, B. Sartori, H. Amenitsch, S. F. Retta and P. P. Pompa, Platinum nanozymes recover cellular ROS homeostasis in an oxidative stress-mediated disease model, *Nanoscale*, 2016, **8**(6), 3739–3752.
34 C. N. Loynachan, M. R. Thomas, E. R. Gray, D. A. Richards, J. Kim, B. S. Miller, J. C. Brookes, S. Agarwal,

V. Chudasama, R. A. McKendry and M. M. Stevens, Platinum Nanocatalyst Amplification: Redefining the Gold Standard for Lateral Flow Immunoassays with Ultrabroad Dynamic Range, *ACS Nano*, 2018, **12**(1), 279–288.

35 X. Jin, L. Chen, Y. Zhang, X. Wang and N. Zhou, A lateral flow strip for on-site detection of tobramycin based on dual-functional platinum-decorated gold nanoparticles, *Analyst*, 2021, **146**(11), 3608–3616.

36 L. Zhu, Z. Lv, Z. Yin, M. Li and D. Tang, Digital multimeter-based point-of-care immunoassay of prostate- specific antigen coupling with a flexible photosensitive pressure sensor, *Sens. Actuators, B*, 2021, **343**, 130121.

37 E. Hornberger, V. Mastronardi, R. Brescia, P. P. Pompa, M. Klingenhof, F. Dionigi, M. Moglianetti and P. Strasser, Seed-Mediated Synthesis and Catalytic ORR Reactivity of Facet-Stable, Monodisperse Platinum Nano-Octahedra, *ACS Appl. Energy Mater.*, 2021, **4**(9), 9542–9552.

38 M. Moglianetti, D. Pedone, P. Morerio, A. Scarsi, P. Donati, M. Bustreo, A. Del Bue and P. P. Pompa, Nanocatalyst-Enabled Physically Unclonable Functions as Smart Anticounterfeiting Tags with AI-Aided Smartphone Authentication, *ACS Appl. Mater. Interfaces*, 2022, **14**(22), 25898–25906.

39 M. Moglianetti, J. Solla-Gullón, P. Donati, D. Pedone, D. Debellis, T. Sibillano, R. Brescia, C. Giannini, V. Montiel, J. M. Feliu and P. P. Pompa, Citrate-Coated, Size-Tunable Octahedral Platinum Nanocrystals: A Novel Route for Advanced Electrocatalysts, *ACS Appl. Mater. Interfaces*, 2018, **10**(48), 41608–41617.

40 V. Mastronardi, J. Kim, M. Veronesi, T. Pomili, F. Berti, G. Udayan, R. Brescia, J. S. Diercks, J. Herranz, T. Bandiera, K. A. Fichthorn, P. P. Pompa and M. Moglianetti, Green chemistry and first-principles theory enhance catalysis: synthesis and 6-fold catalytic activity increase of sub-5 nm Pd and Pt@Pd nanocubes, *Nanoscale*, 2022, **14**(28), 10155–10168.

41 C. Parolo, A. Sena-Torralba, J. F. Bergua, E. Calucho, C. Fuentes-Chust, L. Hu, L. Rivas, R. Álvarez-Diduk, E. P. Nguyen, S. Cinti, D. Quesada-González and A. Merkoçi, Tutorial: design and fabrication of nanoparticle-based lateral-flow immunoassays, *Nat. Protoc.*, 2020, **15**(12), 3788–3816.

42 H. Kawasaki, H. Suzuki, M. Maekawa and T. Hariyama, Combination of the NanoSuit method and gold/platinum particle-based lateral flow assay for quantitative and highly sensitive diagnosis using a desktop scanning electron microscope, *J. Pharm. Biomed. Anal.*, 2021, **196**, 113924.

43 L. Napione, Integrated Nanomaterials and Nanotechnologies in Lateral Flow Tests for Personalized Medicine Applications, *Nanomaterials*, 2021, **11**(9), 2362.

44 V. G. Panferov, I. V. Safenkova, A. V. Zherdev and B. B. Dzantiev, Urchin peroxidase-mimicking Au@Pt nanoparticles as a label in lateral flow immunoassay: impact of nanoparticle composition on detection limit of Clavibacter michiganensis, *Microchim. Acta*, 2020, **187**(5), 268.

45 J. Zhang, L. Tang, Q. Yu, W. Qiu, K. Li, L. Cheng, T. Zhang, L. Qian, X. Zhang and G. Liu, Gold-platinum nanoflowers as colored and catalytic labels for ultrasensitive lateral flow MicroRNA-21 assay, *Sens. Actuators, B*, 2021, **344**, 130325.

46 H. Kawasaki, H. Suzuki, K. Furuhashi, K. Yamashita, J. Ishikawa, O. Nagura, M. Maekawa, T. Miwa, T. Tandou and T. Hariyama, Highly Sensitive and Quantitative Diagnosis of SARS-CoV-2 Using a Gold/Platinum Particle-Based Lateral Flow Assay and a Desktop Scanning Electron Microscope, *Biomedicines*, 2022, **10**(2), 447.

47 P. Cai, R. Wang, S. Ling and S. Wang, A high sensitive platinum-modified colloidal gold immunoassay for tenuazonic acid detection based on monoclonal IgG, *Food Chem.*, 2021, **360**, 130021.

48 L. Dou, Y. Bai, M. Liu, S. Shao, H. Yang, X. Yu, K. Wen, Z. Wang, J. Shen and W. Yu, 'Three-To-One' multi-functional nanocomposite-based lateral flow immunoassay for label-free and dual-readout detection of pathogenic bacteria, *Biosens. Bioelectron.*, 2022, **204**, 114093.

49 C. Zhang, J. Hu, X. Wu, J. Shi and B. D. Hammock, Development of the Au@Pt-Labeled Nanobody Lateral-Flow Nanozyme Immunoassay for Visual Detection of 3-Phenoxybenzoic Acid in Milk and Lake Water, *ACS Agric. Sci. Technol.*, 2022, **2**(3), 573–579.

50 M. Broto, M. M. Kaminski, C. Adrianus, N. Kim, R. Greensmith, S. Dissanayake-Perera, A. J. Schubert, X. Tan, H. Kim, A. S. Dighe, J. J. Collins and M. M. Stevens, Nanozyme-catalysed CRISPR assay for preamplification-free detection of non-coding RNAs, *Nat. Nanotechnol.*, 2022, **17**(10), 1120–1126.

51 A. Scarsi, D. Pedone and P. P. Pompa, A dual-color plasmonic immunosensor for salivary cortisol measurement, *Nanoscale Adv.*, 2023, **5**(2), 329–336.

52 T. Pomili, F. Gatto and P. P. Pompa, A Lateral Flow Device for Point-of-Care Detection of Doxorubicin, *Biosensors*, 2022, **12**(10), 896.

53 A. Charbaji, H. Heidari-Bafroui, C. Anagnostopoulos and M. Faghri, A New Paper-Based Microfluidic Device for Improved Detection of Nitrate in Water, *Sensors*, 2021, **21**(1), 102.

54 M. H. Carlsen, B. L. Halvorsen, K. Holte, S. K. Bøhn, S. Dragland, L. Sampson, C. Willey, H. Senoo, Y. Umezono, C. Sanada, I. Barikmo, N. Berhe, W. C. Willett, K. M. Phillips, D. R. Jacobs and R. Blomhoff, The total antioxidant content of more than 3100 foods, beverages, spices, herbs and supplements used worldwide, *Nutr. J.*, 2010, **9**(1), 3.

55 R. Blomhoff, M. H. Carlsen, L. F. Andersen and D. R. Jacobs, Health benefits of nuts: potential role of antioxidants, *Br. J. Nutr.*, 2006, **96**(S2), S52–S60.

56 M. V. Eberhardt, C. Y. Lee and R. H. Liu, Antioxidant activity of fresh apples, *Nature*, 2000, **405**(6789), 903–904.

57 J. W. Finley, A.-N. Kong, K. J. Hintze, E. H. Jeffery, L. L. Ji and X. G. Lei, Antioxidants in Foods: State of the Science Important to the Food Industry, *J. Agric. Food Chem.*, 2011, **59**(13), 6837–6846.